Chapter 2
Uniform Sampling of Rotations for Discrete and Continuous Learning of 2D Shape Models

Xavier Perez-Sala
Universitat Politècnica de Catalunya, Spain & Computer Vision Center of Barcelona, Spain

Laura Igual
Universitat de Barcelona, Spain & Computer Vision Center of Barcelona, Spain

Sergio Escalera
Universitat de Barcelona, Spain & Computer Vision Center of Barcelona, Spain

Cecilio Angulo
Universitat Politècnica de Catalunya, Spain

ABSTRACT

Different methodologies of uniform sampling over the rotation group, SO(3), for building unbiased 2D shape models from 3D objects are introduced and reviewed in this chapter. State-of-the-art non uniform sampling approaches are discussed, and uniform sampling methods using Euler angles and quaternions are introduced. Moreover, since presented work is oriented to model building applications, it is not limited to general discrete methods to obtain uniform 3D rotations, but also from a continuous point of view in the case of Procrustes Analysis.

INTRODUCTION

Two-dimensional shape models are able to change their shape according to a labeled training set. A shape is composed by a finite set of landmarks whose geometrical information remains unchanged when the shape suffers from rigid transformations. Common 2D shape models (e.g. Point Distribution Models, Active Shape Models) have been successfully applied to solve several problems in Computer Vision, such as face tracking, object recognition, and image segmentation. Usually, these models are learned from a discrete set of 2D shapes once the rigid transformations are removed by aligning the training set, i.e., applying Procrustes Analysis (PA). However, PA is

DOI: 10.4018/978-1-4666-2672-0.ch002

sensible to incomplete and biased set of views of the objects in the training set. In order to solve this problem, examples of 3D objects can be used in two ways: on the one hand, 3D objects are used to extract uniform 2D views to be aligned by standard PA; on the other hand, Continuous Procrustes Analysis (CPA) is used to learn all 3D rigid transformations directly from the 3D examples. In the past, such techniques could only be applied to a limited number of objects, since the most part of databases were storing two-dimensional information. However, recently many 3D databases, as well as 2D databases with three-dimensional information, have become available because of the market release of low cost depth cameras. It is illustrated in Figure 1 how 2D data could be extracted from 3D information provided for this kind of cameras. Different approaches to achieve non biased 2D shape models from 3D data will be explained and discussed along this Chapter.

Uniform sampling of 3D objects is considered a key step when building unbiased 2D shape models. Frequently, Euler angles are used to define three dimensional rotations; however, Euler angles suffer from known problems like gimbal lock or non-uniform rotations (Kuffner, 2004). The main part of this Chapter will be devoted to discuss different configurations to parameterize 3D rotations: usual non-uniform rotations and uniform sampling alternatives using quaternions and Euler angles.

2D shape models are also able to modify their shape in a non-rigid mode, consistent with shape deformations in the training set. The extraction process for non-rigid variations is outlined in the next section; however, deformable models are not addressed in this research, though they could be a direct extension.

BACKGROUND

Building 2D shape models will be the main goal when generating and analyzing uniform rotations. From this perspective, construction of statistical models will be introduced and, specifically, the Procrustes Analysis (PA) technique is described. PA is an important step in model building, as well as it is closely related with the continuous approach of uniform sampling.

2D Shape Models

Two-dimensional shape models are statistical models which are able to modify their shape according to the different transformations present

Figure 1. (left) Image sequence obtained from a depth camera; (middle) 3D skeletons extracted using Kinect© for Windows SDK; (right) 5 cameras, randomly distributed around the 3D skeleton, are displayed.

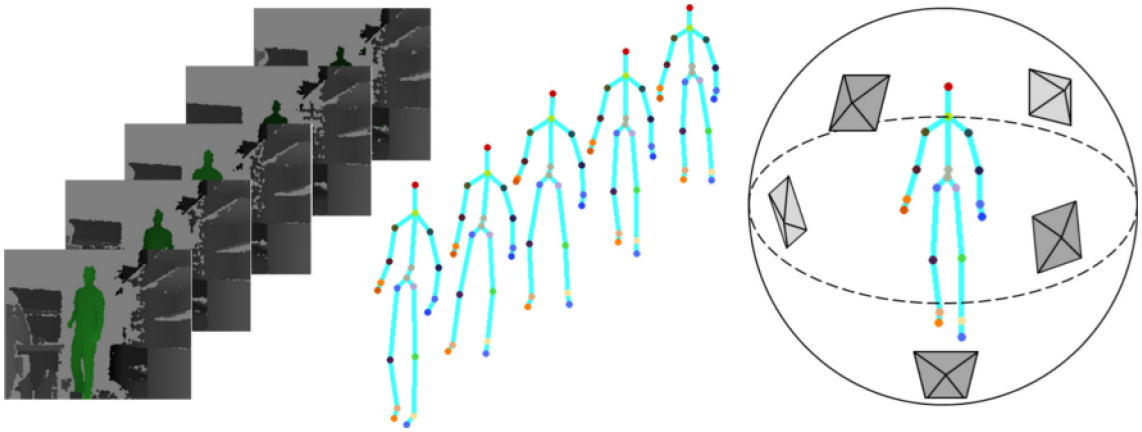

in a training set (Cootes & Taylor, 2001). The training set should be labeled with landmark correspondences across all the training shapes, where a shape is defined as a finite set of landmarks whose geometrical information remains unchanged when the shape suffers rigid transformations.

The building process for 2D shape models requires a set of training shapes composed by a number l of landmarks, where each landmark should be consistently labeled, representing the same anatomical location across all training shapes. The building process starts by removing rigid transformations in the training set using Procrustes Analysis (PA), which minimizes the least squares error between landmarks from training shapes and the mean shape m, which is also computed.

After aligning the shapes, each *d*-dimensional training shape is represented as a point $s \in \mathbb{R}^{dl}$, as well as the mean shape $m \in \mathbb{R}^{dl}$. In the case of three dimensional shapes, each point has the form $s = (x_1, y_1, z_1, ..., x_l, y_l, z_l)$. In the second step of model building, it is assumed that all points represented in the space $\mathbb{R}^{dl}$ follow a Gaussian probability density function. Eigenvectors and eigenvalues are computed using Principal Component Analysis (PCA), and the set of most informative eigenvectors is used as the basis of a subspace *B*, which summarizes the non-rigid variations among all the training shapes. The percentage of information explained using the subspace *B* is selected by choosing the number *r* of ordered basis. Columns in matrix $B \in \mathbb{R}^{dl \times r}$ are the most informative eigenvectors, each one describing a principal mode of variation in the training set.

The last step of the process is shape representation using the computed information. Following the Point Distribution Model (PDM) approach, new shapes can be represented as $s = m + Bc$; where $c \in \mathbb{R}^{l \times r}$ is a vector weighting each basis over the shape *s*. Hence, an infinite number of shapes can be created by modifying parameters in *c*. Moreover, limits over *c* guarantee that new shapes will follow the variations present in the training set. Usually, *c* parameters are limited such as $|c_i| < 3\sqrt{\lambda_i}$, where λ_i is the *i*-th eigenvalue, which means that *c* parameters are limited within ± 3 their corresponding standard deviation. Further details are specified in (Cootes & Taylor, 2001).

The most popular techniques using 2D shape models are PDM and Active Shape Models (ASM) (Cootes & Taylor, 2001). Many computer vision problems have been successfully treated by their application: image segmentation (Osher & Paragios, 2003; Mumford & Shah, 1989), object recognition (Ullman & Basri, 1991; Jones & Poggio, 1989), and face tracking (Baker et al., 2004; Dela Torre & Nguyen, 2008; Blanz & Vetter, 1999; Cootes et al., 2001; Gong et al., 2000), among others.

Procrustes Analysis

Rigid registration among different shapes, composed by labeled landmarks, is usually addressed by Procrustes Analysis (PA) (Goodall, 1991). More precisely, it is called Generalized Procrustes analysis (GPA) when more than two shapes are aligned (see Figure 2). GPA minimizes the least squares error between the landmarks of each training shape and a mean shape, while this mean shape is as well estimated:

$$E_1(M, A_1, ..., A_n) = \sum_{i=1}^{n} \left\| A_i D_i - M \right\|_F^2 .$$

PA is used to compute the mean shape $M \in \mathbb{R}^{2 \times l}$ of the training set and the *n* rigid transformations $A_i \in \mathbb{R}^{2 \times 2}$ between the mean shape and each training sample $D_i \in \mathbb{R}^{2 \times 1}$, where *n* is the number of training shapes, *l* is the number of landmarks that compose each shape, and $\|X\|_F^2 = tr\left(X^T X\right)$ designates the square of the

Figure 2. (left) Training set after translation removal; (right) aligned training set (blue points) and the mean shape (red line) using Procrustes analysis

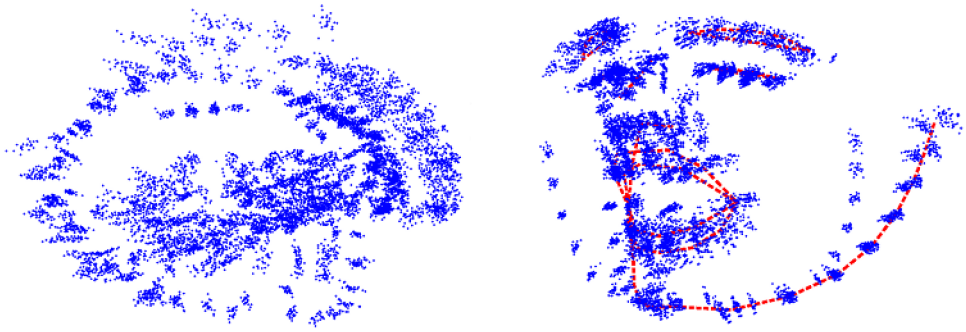

Frobenius norm of a matrix. PA is usually expressed as a vector (Cootes & Taylor, 2001), however E_1 is formulated using matrices for easy comparison with Continuous Procrustes Analysis (CPA), later introduced.

Though analytic solutions exist for training set alignment (Horn, 1987), iterative approaches are commonly used (Eggert et al., 1997; Cootes & Taylor, 2001) because of their intuitiveness and fast convergence. A standard iterative approach proceeds as follows. First of all, shape translations are removed by displacing the centers of gravity of all shapes to the origin. The second step of GPA consists on choosing one training shape as an initial estimate of the mean shape. In the third step, all training shapes are aligned with the estimation of the mean shape. Finally, the mean shape M is re-estimated from the aligned shapes. The algorithm iterates from the third step until convergence of M.

It is known that neither iterative methods nor analytic approaches guarantee the convergence to the global optimal solution. Recent works have proposed more accurate solutions (Bartoli et al., 2010) and new optimization procedures for finding the global optimal solution (Pizarro & Bartoli, 2011).

UNIFORM ROTATIONS

Building 2D shape models from 3D objects databases can be addressed by applying 2D techniques over 2D views, sampled from 3D training examples. Since 2D views from training set can bias the estimation of the shape model, an uniform coverage of all 3D transformations of the objects is needed, which can be addressed from both, discrete and continuous formulations.

Issues, Controversies, and Problems

The final goal of uniform rotations in our domain is obtaining a set of 2D object views, uniformly distributed along all possible rotations of a 3D object. Given a 3D shape and a virtual camera with a fixed point of view, it could be achieved by rotating the three-dimensional object over the rotation group SO(3) in a uniform way.

The Special Orthogonal group in three dimensions, SO(3), forms a group with its action being the composition of rotations. Each rotation is a linear transformation that preserves vectors length and space orientation. SO(3) is not only a group, but also a manifold, which makes it a Lie group. Moreover, this manifold has the topology of real 3-dimensional projective space $\mathbb{RP}^3$.

In order to appreciate the transformations suffered for a 3D object by the rotations, its minimal representation is the composition of two unit 3D vectors from the origin (see Figure 3). Our problem about uniform sampling of rotations, therefore, can be understood as the uniform distribution of couples of unit vectors into the unit 2-sphere, so that both vectors follow a uniform density function over the sphere surface, and the angle represented by the union of both vectors in the sphere surface follows a uniform distribution.

There exist several representations for 3D rotations, the most common of them Euler angles and quaternions. In the following sections different parameterizations for Euler angles and quaternions are presented. Moreover, in order to achieve uniform rotations with the final goal of building 2D shape models, a continuous methodology is also described in the scope of Procrustes Analysis.

Euler Angles

Euler angles represent orientations in the rotation group SO(3) through the composition of three rotations (a, β, γ), each one around a single axis of a basis. The final rotation is obtained multiplying three rotation matrices:

$$R_{xyz} = R_z(\gamma)R_y(\beta)R_x(\alpha)$$

where:

$$R_z(\gamma)\begin{bmatrix}\cos\gamma & -\sin\gamma & 0\\ \sin\gamma & \cos\gamma & 0\\ 0 & 0 & 1\end{bmatrix}$$

$$R_y(\beta)\begin{bmatrix}\cos\beta & 0 & \sin\beta\\ 0 & 1 & 0\\ -\sin\beta & 0 & \cos\beta\end{bmatrix}$$

$$R_x(\alpha)\begin{bmatrix}1 & 0 & 0\\ 0 & \cos\alpha & -\sin\alpha\\ 0 & \sin\alpha & \cos\alpha\end{bmatrix}.$$

Since matrix product is not commutative, different permutations of the axes result in different orientations. There are at least 24 conventions for Euler angles, depending on the chosen Cartesian axes and which order is applied: 3 (*first axis: x, y, z*) × 2 (*second axis*) × 2 (*first axis repetition, or not*) × 2 (*static or rotating axes*) = 3 × 2 × 2× 2 = 24 possibilities.

Nevertheless, all of them suffer the same issues: non-uniform distribution of orientations, singularities, and the gimbal lock problem.

The gimbal lock problem for rotations in the three-dimensional space appears when two out of the three axes are parallel. One degree of freedom is lost and, therefore, only rotations in two-dimensional space are performed. An easy example to understand this issue appears when using the convention Z-Y-Z, i.e., first, a rotation on the *Z-axis* by α angle, followed by a turn on the rotated *Y-axis* of β angle and, finally, a rotation by γ angle on the new *Z-axis*. If $\beta = 0$, it pro-

Figure 3. Rotation of ψ angle between y-axis (vertical arrow) and the union of the couple of unit vectors (dashed), i.e. the shape, in the sphere surface

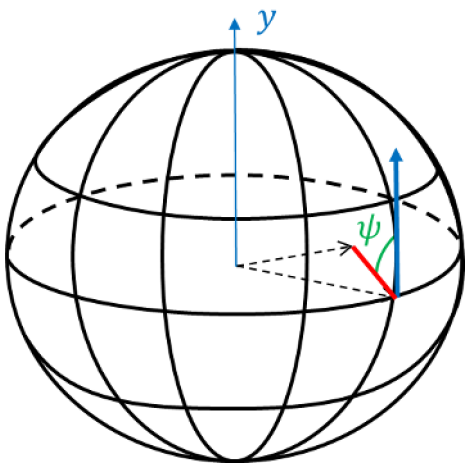

duces a rotation by $\delta_1 = \alpha + \gamma$ angle, only on *Z-axis*. In this case, the system loses a degree of freedom and it is "locked" rotating in a degenerate two-dimensional space. Of course, the same situation occurs when $\beta = \pi$, with a final rotation of $\delta_2 = \alpha - \gamma$ angle around *Z-axis*.

It is a clear example of singularity on Euler angles, where different rotations in SO(3) are mapped onto a single rotation in the Euler representation. In the previous example, the final rotation described by $\beta = 0$ and $\delta_1 = \alpha + \gamma$ could be achieved by any different combination of α and γ, as well as infinity. Other simple example to visualize singularities is the Mercator projection of the globe. In this case, lines representing North and South poles are mapped as single points in the globe. Singularities usually lead to representation problems around its influence area, because small changes in one representation may lead to large changes in other representation.

Hence, points uniformly distributed near the pole lines in the Mercator projection, representing large distances in this representation, will be overrepresented near the North pole or South pole points of the globe. Returning to the Euler angles example, rotations with $\beta \approx 0$ or $\beta \approx \pi$ will be overrepresented, resulting in a non-uniform distribution of 3D orientations.

Perhaps other Euler angles standards, like X-Y-Z convention, make more difficult to guess the final orientations. However, for the X-Y-Z convention example (shown in Figure 4(left)) the distribution of orientations are not uniform, focusing rotations in the poles of the unit sphere. Angle ranges chosen to perform the experiment in Figure 4(left) are the domains for Euler angles: $\alpha, \gamma = \mathcal{U}(-\pi, \pi]$ and $\beta = \mathcal{U}\left[-\frac{\pi}{2}, \frac{\pi}{2}\right]$, where $\mathcal{U}$ means that angles can take values uniformly distributed on the interval.

It was previously stated that a couple of vectors is the minimum expression of a shape where 3D rotations can be appreciated. Hence, the performance of different approaches when sampling rotations over SO(3) will be checked by observing their application over a couple of unit vectors (i.e. the shape). Our goal is to obtain uniform distribution of shapes into the unit 2-sphere.

Shoemake (1992) stated that coordinates $\{x,y,z\}$ of a vector uniformly distributed on a sphere are also uniformly distributed between their limits $(x, y, z \in [-1, +1]$ in the case of the unit sphere). Therefore, 2D shape rotations over the unit sphere surface are uniformly distributed while one of the vectors that compose the shape has its components uniformly distributed between the limits of the unit sphere.

The third rotation of the shape is referred to the relative change of orientation between the pair of vectors that compose the shape. 3D shape rotations are uniformly distributed while the ψ angle between the Y-axis and the line painted by the couple of vectors in the sphere surface (illustrated in Figure 3) follows as well a uniform distribution.

It is shown in Figure 5 (lower row) that angle follows a uniform distribution. However, Euler angles do not perform a uniform distribution of rotations because $\{x,y,z\}$ components of rotated vectors have a non-uniform distribution (Figure 5, upper row). Qualitative results (Figure 4(left)) also indicated a non-uniform distribution of the vectors, since the number of rotations over the poles is visually higher than for the rest of the unit sphere. However, it is possible to compensate non-uniformity depending on the Euler angles convention. Uniformly randomized orientations using X-Y-Z convention (Figure 6 (left)) could be achieved with $\alpha, \gamma = \mathcal{U}(-\pi, \pi]$, $z = \mathcal{U}(-1 + 1)$ and $\beta = \sin^{-1}(z)$; when the Z-Y-Z convention is used (Figure 7 (right)), uniformly distributed orientations could be achieved with $\alpha, \gamma = \mathcal{U}(-\pi, \pi]$, $z = \mathcal{U}(-1 + 1)$ and $\beta = \cos^{-1}(z)$.

Following the criteria established in the previous example, Figure 7 indicates a uniform distri-

Figure 4. Sampling of 5000 rotations of a couple of unit vectors: (left) uniform sampling of Euler angles following the x-y-z convention; (right) uniform sampling of quaternion parameters using the method presented in (Shoemake, 1992)

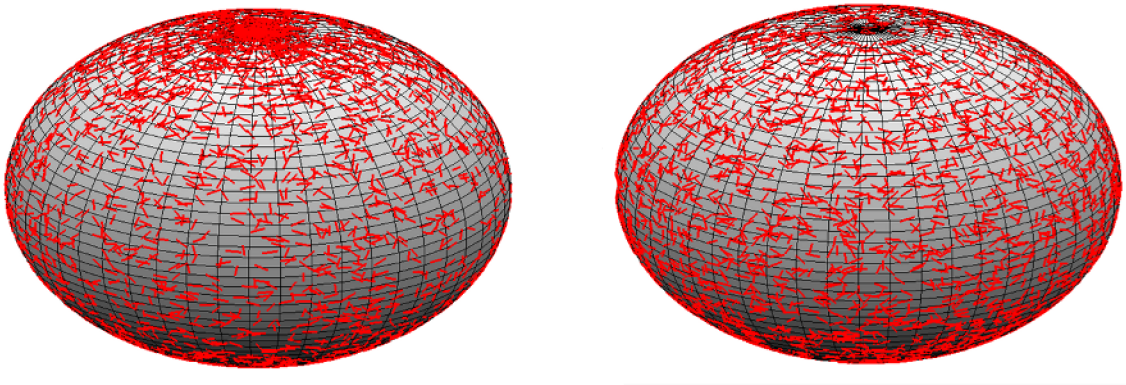

bution over the sphere because each coordinate of the rotated vectors is uniformly distributed (Figure 7, upper row); moreover, angle (Figure 7, lower row) shows that relative rotations between two vectors painted in the sphere are uniform as well.

Quaternions

Quaternions were conceived by Hamilton (1853) as extended complex numbers $q = [a, b\boldsymbol{i}, c\boldsymbol{j}, d\boldsymbol{k}]$. Each unit quaternion can be interpreted as a point in the unit 3-sphere $S^3 \in \mathbb{R}^4$, which represents a rotation on SO(3). For any unit quaternion $q = \boldsymbol{q}_0 + q = \cos(\theta / 2) + \hat{\boldsymbol{u}} \sin(\theta / 2)$ and for any vector $\boldsymbol{v} \in \mathbb{R}^3$, the action of the triple product $q_{v'} = qq_v q^*$ may be interpreted geometrically as a rotation of the vector $\boldsymbol{v}$ through an angle θ around $\hat{\boldsymbol{u}}$ as the axis of rotation (Kuipers, 1999), where a unit quaternion is defined as $|q| = |q^*| = \sqrt{q^* q} = 1$, q^* is the quaternion conjugate, and $q_v = [0, v]$ is the vector $\boldsymbol{v}$ expressed as a pure quaternion, i.e. a quaternion whose scalar part is 0.

Following quaternion algebra (Lerios, 1995), an equivalent rotation can be represented in matrix formulation as $q_{v'} = qq_v q^* = R_q q_v$, with:

$$R_q = \begin{pmatrix} a^2 + b^2 + c^2 + d^2 & 0 & 0 & 0 \\ 0 & a^2 + b^2 - c^2 - d^2 & 2bc + 2ad & 2bd - 2ac \\ 0 & 2bc - 2ad & a^2 - b^2 + c^2 - d^2 & 2cd + 2ab \\ 0 & 2bd + 2ac & 2cd - 2ad & a^2 - b^2 - c^2 + d^2 \end{pmatrix}.$$

Figure 5. Non-uniform distribution of the rotated vector parameters (up) with the mean of all distributions (horizontal line) and distribution of spherical coordinates (down) with the mean of ψ distribution (horizontal line), using Euler angles following the x-y-z convention.

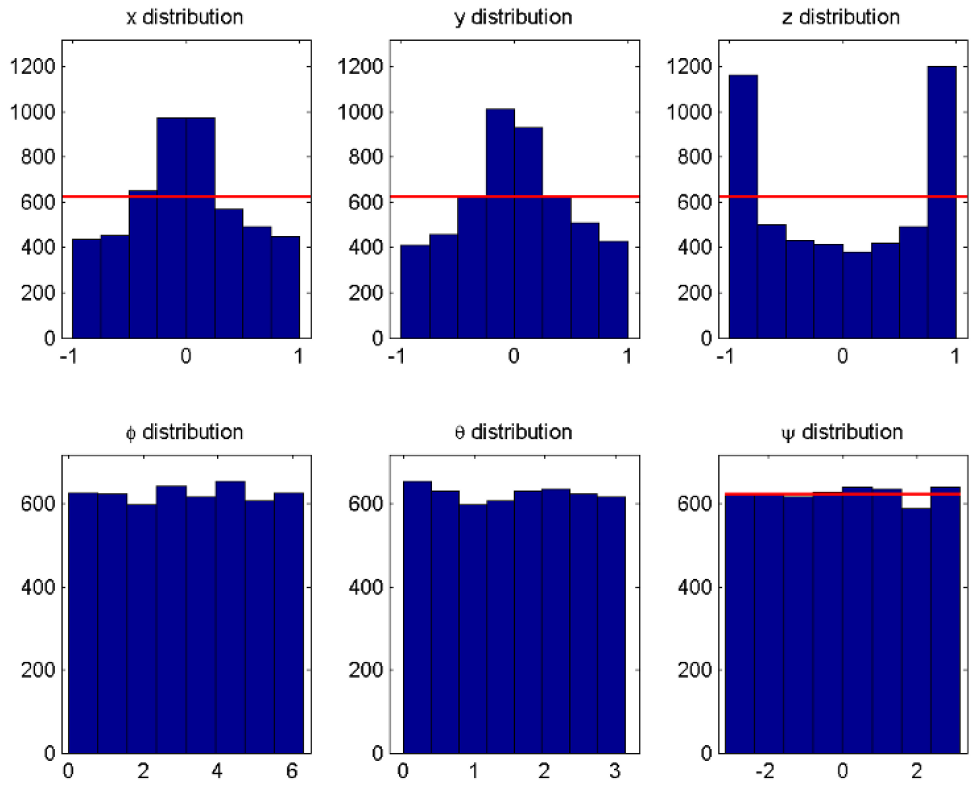

Since $q = [a, b, c, d]$ is a unit quaternion such that $\|q\| = q^* q = a^2 + b^2 + c^2 + d^2 = 1$, R_q canbe simplified to:

$$R_q = \begin{pmatrix} |q|^2 & 0 & 0 \\ 0 & |q|^2 - 2(c^2 + d^2) & 2(bc - ad) \\ 0 & 2(bc + ad) & |q|^2 - 2(b^2 + d^2) \\ 0 & 2(bd - ac) & 2(cd + ab) \end{pmatrix} ==$$

$$\begin{pmatrix} 1 & 0 & 0 \\ 0 & 1 - 2(c^2 + d^2) & 2(bc - ad) \\ 0 & 2(bc + ad) & 1 - 2(b^2 + d^2) \\ 0 & 2(bd - ac) & 2(cd + ab) \end{pmatrix}$$

$$\begin{pmatrix} 0 & 0 \\ 2(bc - ad) & 2(bd + ac) \\ |q|^2 + 2(b^2 + d^2) & 2(cd - ab) \\ 2(cd + ab) & |q|^2 - 2(b^2 + c^2) \end{pmatrix} = \begin{pmatrix} 1 & 0 \\ 0 & Q \end{pmatrix},$$

$$\begin{pmatrix} 0 \\ 2(bd + ac) \\ 2(cd - ab) \\ 1 - 2(b^2 + c^2) \end{pmatrix}$$

which satisfies the properties of rotation matrices (Lerios, 1995). An equivalent matrix is presented in (Shoemake, 1991) using a different order of the quaternion components

Figure 6. Sampling of 5000 rotations of a couple of unit vectors by non-uniform sampling of Euler angles: (left) following x-y-z convention to achieve uniform rotations; and (right) following the z-y-z convention

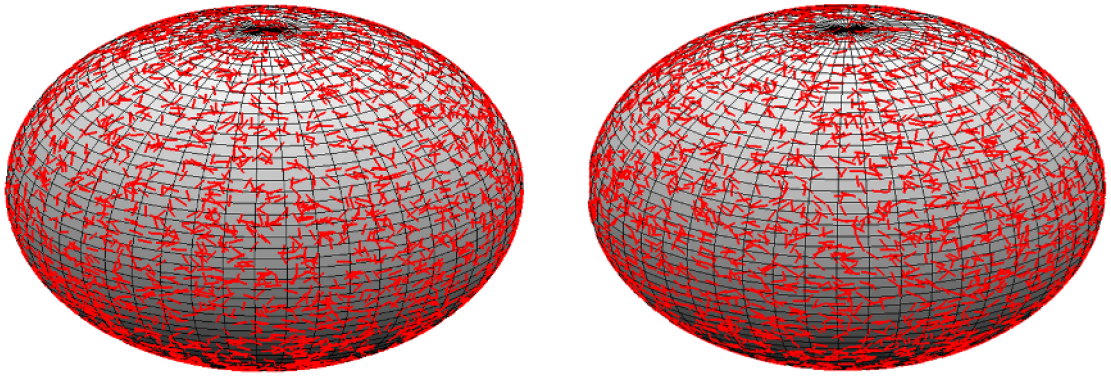

$q = [x, y, z, w] = [b, c, d, a]$. Moreover, to avoid unnecessary calculus and vector-quaternion conversions, vector rotations using quaternions could be calculated by the product $v' = Qv$, where $Q \in \mathbb{R}^{3\times3}$ and $v' \in \mathbb{R}^{3\times1}$ is the rotated vector.

The axis-angle interpretation shows that quaternions are composed by only one rotation and, therefore, they do not suffer from the gimbal lock problem, though opposite quaternions $q = -q$ represent the same rotation. However, not all parameterizations perform uniform rotations despite of the use of quaternions. In the following paragraphs three different parameterizations are considered.

Euler Angles Conversion

Given the difficulty linked to quaternions, the first naïve attempt to present intuitive rotations lies on using a unit quaternion expressed in Euler angles. Nevertheless, a uniform sampling of Euler angles does not perform uniform rotations despite of quaternion conversion, and gimbal lock problem persists.

Given the three Euler angles (α, β, γ), three independent quaternions can be formed:

$$q_x = \left[\cos\left(\frac{\alpha}{2}\right), \left(\sin\left(\frac{\alpha}{2}\right), 0, 0\right)\right],$$

$$q_y = \left[\cos\left(\frac{\beta}{2}\right), \left(0, \sin\left(\frac{\beta}{2}\right), 0\right)\right],$$

$$q_z = \left[\cos\left(\frac{\gamma}{2}\right), \left(0, 0, \sin\left(\frac{\gamma}{2}\right)\right)\right].$$

Similarly to rotation matrices, the joint rotation is represented by the final quaternion

$$q_{xyz} = q_z q_y q_x = \left[a_{xyz}, b_{xyz}, c_{xyz}, d_{xyz}\right],$$

where:

$$a_{xyz} = \cos\left(\frac{\alpha}{2}\right)\cos\left(\frac{\beta}{2}\right)\cos\left(\frac{\gamma}{2}\right) + \sin\left(\frac{\alpha}{2}\right)\sin\left(\frac{\beta}{2}\right)\sin\left(\frac{\gamma}{2}\right),$$

Figure 7. Uniform distribution of the rotated vector parameters (up) with the mean of all distributions (horizontal line) and distribution of spherical coordinates (down) with the mean of ψ distribution (horizontal line), using a uniform sampling distribution of Euler angles following the x-y-z convention

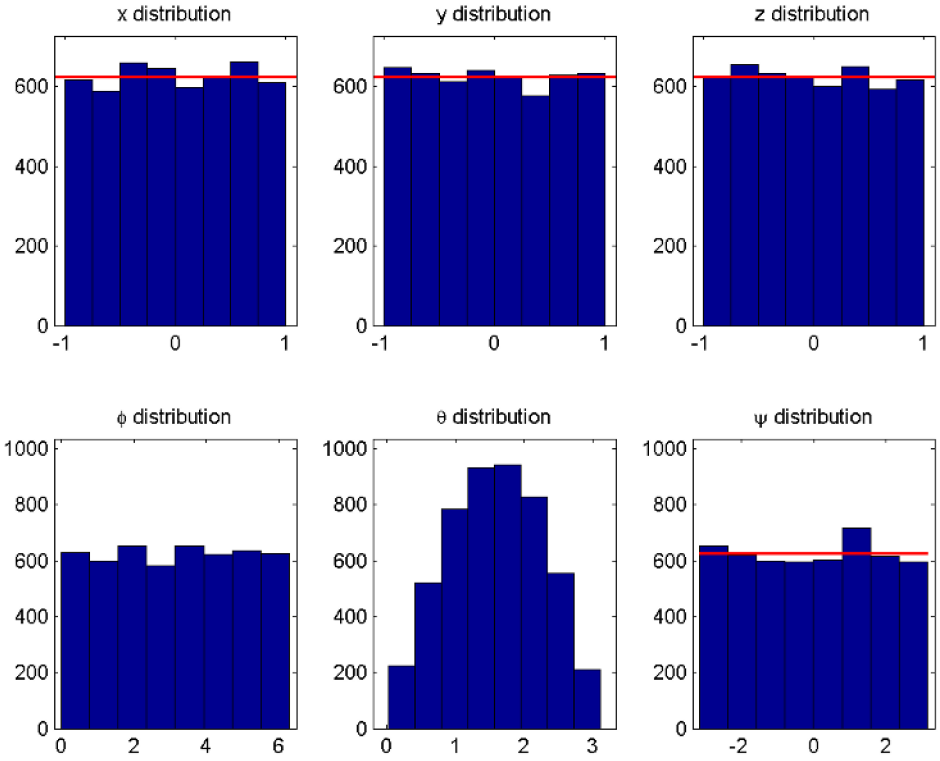

$$b_{xyz} = \sin\left(\frac{\alpha}{2}\right)\cos\left(\frac{\beta}{2}\right)\cos\left(\frac{\gamma}{2}\right) - \cos\left(\frac{\alpha}{2}\right)\sin\left(\frac{\beta}{2}\right)\sin\left(\frac{\gamma}{2}\right),$$

$$c_{xyz} = \cos\left(\frac{\alpha}{2}\right)\sin\left(\frac{\beta}{2}\right)\cos\left(\frac{\gamma}{2}\right) + \sin\left(\frac{\alpha}{2}\right)\cos\left(\frac{\beta}{2}\right)\sin\left(\frac{\gamma}{2}\right),$$

$$d_{xyz} = \cos\left(\frac{\alpha}{2}\right)\cos\left(\frac{\beta}{2}\right)\sin\left(\frac{\gamma}{2}\right) - \sin\left(\frac{\alpha}{2}\right)\sin\left(\frac{\beta}{2}\right)\cos\left(\frac{\gamma}{2}\right).$$

If q_{xyz} is not a unit vector due to numerical drift, it should be normalized such that $\hat{q}_{xyz} = q_{xyz} / \left|q_{xyz}\right|$. Given a uniform sampling of the three parameters, such that $\alpha, \gamma = \mathcal{U}(-\pi, \pi]$ and $\beta = \mathcal{U}\left[-\frac{\pi}{2}, \frac{\pi}{2}\right]$, rotations obtained follow the same distribution as orientations performed using rotation matrices in the previous section. Qualitative results comparing both approaches are presented in Figure 8, where rotations are concentrated onto the poles of the 2-sphere.

As it was performed in previous sections, the uniform distribution of couples of unit vectors onto the unit 2-sphere is checked for the uniformity of {*x,y,z*} coordinates of unit vectors and, in addition, for the uniform distribution of the angle (shown in Figure 2) between the Y-axis and the union joining both vectors.

Figure 8. Sampling of 5000 rotations of a couple of unit vectors by uniform sampling of Euler angles following x-y-z convention, (left) using rotation matrices and (right) using quaternions, based on Euler angles parameterization

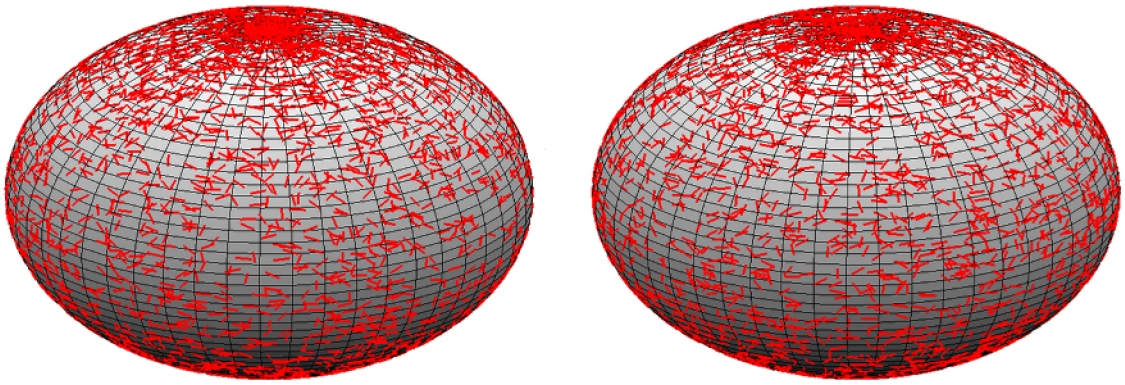

Similarly to Figure 5, rotations performed with quaternions parameterized by Euler angles result in non-uniform rotations. Figure 9 (lower row) shows a uniform distribution over ψ angle, though the vector distribution is not uniform around the sphere S^2 because vector coordinates are not uniformly distributed (Figure 9, upper row). In addition, a parameterization based on Euler angles conversion does not solve the gimbal lock problem.

Axis-Angle Parameterization

In order to avoid previous problems, it is necessary to work with other parameters closely related to quaternion rotations. As it was explained in the beginning of this section, a unit quaternion $q = \boldsymbol{q}_0 + q = \cos(\theta / 2) + \hat{\boldsymbol{u}} \sin(\theta / 2)$ can be expressed as a rotation by θ angle around $\hat{\boldsymbol{u}}-$ axis. Since the uniform sampling of becomes in uniform rotations over $\hat{\boldsymbol{u}}-$axis, the intuitive attempt is to perform these 2D rotations over a set of uniformly distributed $\hat{\boldsymbol{u}}$ on the unit sphere S^2. The process considered to obtain a uniform distribution of unit vectors $\hat{\boldsymbol{u}} = \left[u_x, u_y, u_z\right]$ in the unit 2-sphere (Shoemake, 1992) is illustrated in Figure10.

Given three random variables θ, u_z, ρ, rotations are performed by the unit quaternion q, where $\theta = \mathcal{U}(0, 2\pi)$ and $\hat{u}$ are defined as:

$$u_z = \mathcal{U}\left(-1+1\right),$$

$$\rho = \mathcal{U}(0, 2\pi),$$

$$z^2 + r^2 = 1 \rightarrow r = \sqrt{1 - z^2},$$

$$u_x = r\cos\rho,$$

$$u_x{}^2 + u_y{}^2 = r^2 \rightarrow r^2((\sin\rho)^2 + (\cos\rho)^2) = r^2 \rightarrow (r\sin\rho)^2 + (r\cos\rho)^2 = r^2,$$

$$u_y = \sqrt{(r\sin\rho)^2} = \pm r\sin\rho.$$

Therefore, two quaternions are created with opposite $\hat{\boldsymbol{u}}$ axis for each three random values. Qualitative results in Figure 11 show that the composition of uniform rotation axis $\hat{\boldsymbol{u}}$ and uniform angle θ does not perform a uniform distribution of unit quaternions.

Figure 9. Non-uniform distribution of the rotated vector parameters (up) with the mean of all distributions (horizontal line) and distribution of spherical coordinates (down) with the mean of ψ distribution (horizontal line), using Euler angles-to-quaternion conversion

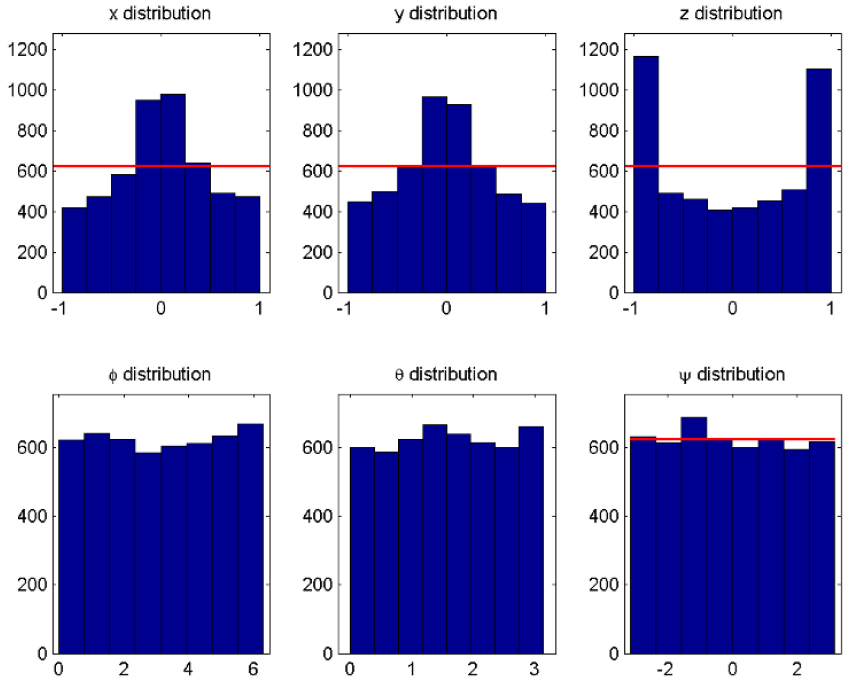

Figure 10. To achieve uniformly distributed unit vectors $\hat{\mathbf{u}}$ in the unit 2-sphere, u_z takes values along the diameter following a uniform distribution, $u_z = \mathcal{U}(-1+1)$; and u_x, u_y are distributed on the circle (green) of radius r (red), which cuts the sphere by u_z (blue)

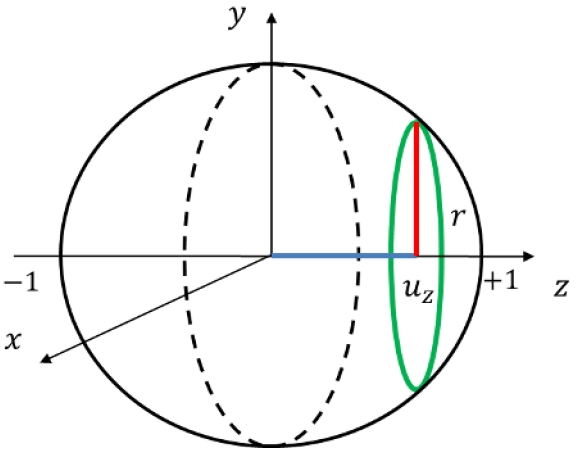

The distribution of vector components (Figure 12, upper row) when rotated using the previously created random quaternions are non-uniform, which means that neither rotations are uniform onto the unit 2-sphere, nor orientations over the sphere surface measured by angle (Figure 12, lower row).

Parameters Defined in (Shoemake, 1992)

Finally, taking inspiration as well from a composition of rotations, a direct method is presented in (Shoemake, 1992), where the four quaternion parameters are calculated through the use of three random variables. Figure 4 (right) shows the correctness of this method, obtaining uniform three-dimensional orientations. Similarly to the method proposed in (Yershova et al., 2010), Shoemake's approach computes unit random quaternions addressing the problem from the subgroup algorithm.

Figure 11. Sampling of 5000 rotations of a couple of unit vectors using random quaternions created from a uniform sampling of θ and uniformly distributed $\hat{\mathbf{u}}$ – axis

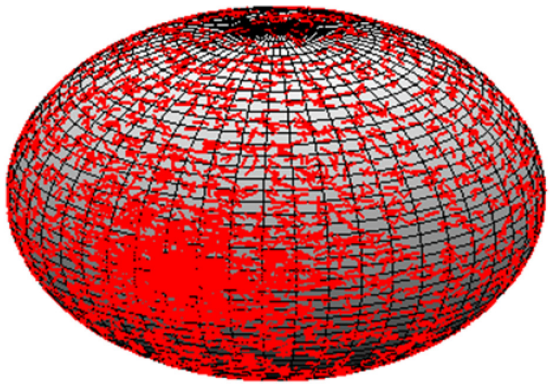

If all 3D rotations in the space compose a group, a subgroup $q = (c, 0, 0, s)$ of this group is constituted by planar rotations around the Z-axis, and cosets $q = (w, x, y, 0)$ of this subgroup are rotations pointing Z-axis in different directions. Following the subgroup algorithm (Diaconis & Shahshahani, 1987), a uniformly distributed element of the complete group can be achieved by the multiplication of a uniformly distributed element from the subgroup with a uniformly distributed *coset*:

$$\mathcal{U}([c,0,0,s])\mathcal{U}([w,x,y,0]) = \mathcal{U}[[cw, cx+sy, -sx+cy, sw]].$$

Given three independent random variables $X_0, X_1, X_2 \in \mathcal{U}(0,1)$, random unit quaternions $q = [\cos\theta_2 r_2, \sin\theta_1 r_1, \cos\theta_1 r_1, \sin\theta_2 r_2]$ are computed, where:

$$\theta_1 = 2\pi X_1,$$

$$\theta_2 = 2\pi X_2,$$

$$r_1 = \sqrt{1 - X_0},$$

$$r_2 = \sqrt{X_0}.$$

Results exposed in Figure 13 indicate a uniform distribution over the sphere because each coordinate $\{x,y,z\}$ of the rotated vector is uniformly distributed (Figure 13, upper row). Moreover, ψ angle distribution (Figure 13, lower row) shows that relative rotations between the Y-axis and the union of the couple of vectors in the sphere follow a uniform distribution as well.

Continuous Procrustes Analysis

In the particular field of learning 2D shape models, an alternative to discrete model building is proposed in (Igual & De la Torre, 2010), where 2D discrete techniques are extended to be applied over 3D models in a continuous form. Continuous Procrustes Analysis (CPA) is presented as a competitive alternative to Generalized Procrustes Analysis (GPA) when 3D models are available.

Shape models learned using GPA (Figure 14, left) could be biased by a non-uniform sampling of the 2D views of the 3D examples. This issue, the computational cost, and large amount of data associated to the uniform sampling of 3D transformations are solved by CPA (Figure 14, right). CPA gives a closed form solution for the learning of 2D models directly from a 3D training set, incorporating the information of all 3D rigid transformations.

CPA minimizes the least-squared error between the 2D projections of 3D landmarks of each training shape and a 2D mean shape, while this mean shape is also estimated. Let $\Omega = \{\omega = (\phi, \theta, \psi)\} \in \mathbb{R}^3$ be the set of 3D rotations, where ω are the Euler angles and the Haar measure is $d\omega = \sin\theta d\phi d\theta d\psi$. CPA minimizes the following energy functional:

Figure 12. Non-uniform distribution of the rotated vector parameters (up) with the mean of all distributions (horizontal line) and distribution of spherical coordinates (down) with the mean of ψ distribution (horizontal line), using random quaternions composed by random uniform rotation axis $\hat{\mathbf{u}}$ and uniform angle θ

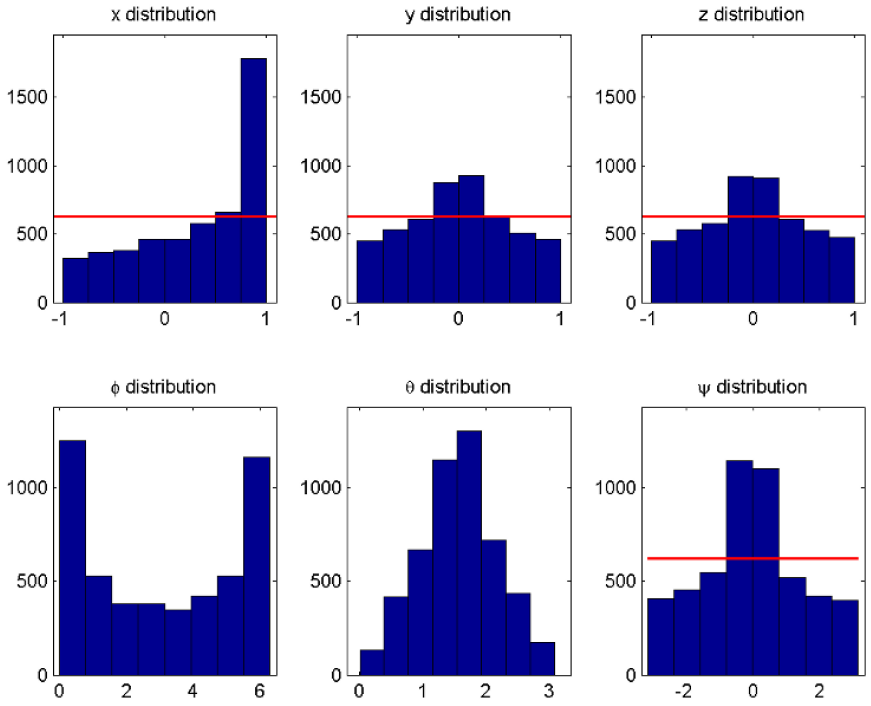

$$E_2(M, A_1, ..., A_n) = \sum_{i=1}^{n} \int_{\Omega} F_2(M, A_i(\omega)) d\omega = \sum_{i=1}^{n} \int_{\Omega} \left\| PR(\omega) D_i - A_i(\omega) M \right\|_F^2 d\omega.$$

CPA computes the two-dimensional mean shape $M \in \mathbb{R}^{2\times 1}$ of the training set and the n rigid transformations $A_i(\omega) \in \mathbb{R}^{2\times 2}$ between the mean shape and the orthographic projection $P \in \mathbb{R}^{2\times 3}$ of each training sample $D_i \in \mathbb{R}^{3\times 1}$, which is rotated over all possible Euler angles of the domain Ω, by the rotation matrix $R \in \mathbb{R}^{3\times 3}$ As in the previous section, n is the number of training shapes and l is the number of landmarks that form each shape. The matrix P describes the orthographic projection onto the plane Z=0, defined as:

$$P = \begin{pmatrix} 1 & 0 & 0 \\ 0 & 1 & 0 \end{pmatrix}.$$

The CPA functional $E_2(M, A_1, ..., A_n)$ is similar to the energy function $E_1(M, A_1, ..., A_n)$ from GPA; however, there are three main differences: first, E_2 is a continuous formulation where discrete sums are extended to integrals; the second difference relies on the 2D views used in E_2, which depend directly on the 3D structure of the training examples D_i and the 3D transformation parameters $R(\omega)$; and the third difference is that, A_i in E_1 are variables, whereas in E_2 are functions depending on Euler angles ω.

Note that uniform rotations are achieved by $R(\omega)$. Since using Haar measure $d\omega$, an invariant integral for functions on the rotation group SO(3)

Figure 13. Uniform distribution of the rotated vector parameters (top) with the mean of all distributions (horizontal line) and distribution of spherical coordinates (down) with the mean of ψ distribution (horizontal line), using the methodology proposed in (Shoemake 1992)

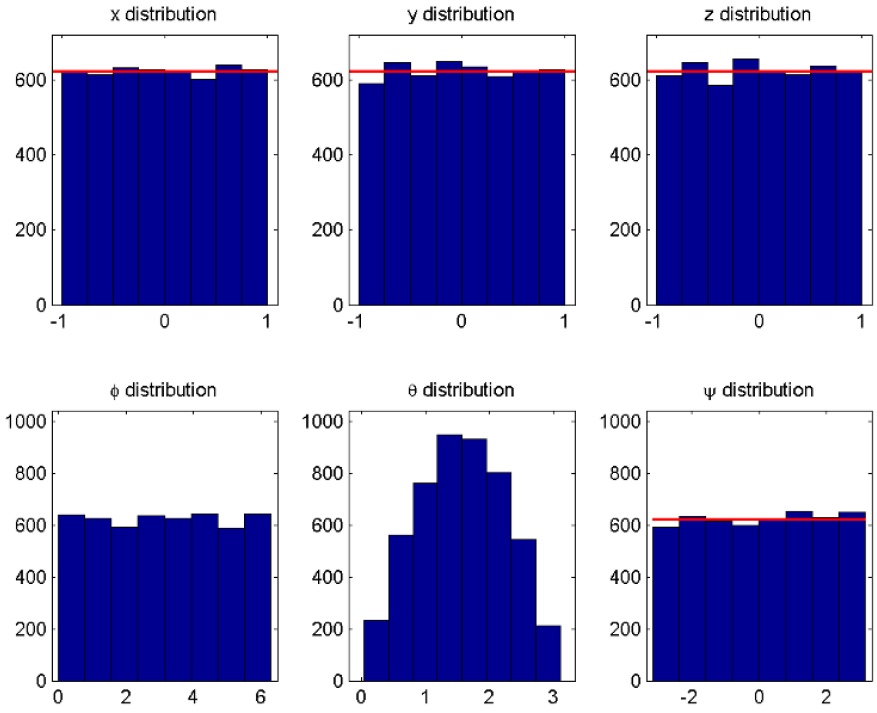

is obtained (Naimark, 1964), despite of the use of Euler angles. Therefore, the problem of discrete non-uniform distribution discussed above is avoided in the integral definition.

SOLUTIONS AND RECOMMENDATIONS

The final goal to achieve uniform rotations is obtaining a set of 2D object views uniformly distributed along all possible rigid transformations of a 3D object. To test the presented methodologies, a couple of unit vectors is rotated into the unit 2-sphere. Distribution of rotations is considered uniform when each rotated vector follows a uniform distribution over the sphere surface and, moreover, a uniform distribution of the angle between the vertical axis and the union of the couple of vectors in the sphere surface. Since Shoemake (1992) stated that $\{x,y,z\}$ coordinates of a vector uniformly distributed on a sphere are also uniformly distributed between their limits (into the unit sphere: $x, y, z \in [-1, +1]$), the correct distribution of vectors over the sphere surface is checked by the distribution of its components. In addition, distribution function of the angle between both vectors onto the sphere surface is tested by the uniformity of ψ angle, as illustrated in Figure 2.

Results presented in the previous section show, first of all, that uniform sampling of Euler angles does not result in uniform rotations when three Euler angles take values between the common limits: $\alpha, \gamma = \mathcal{U}(-\pi, \pi]$ and $\beta = \mathcal{U}\left[-\frac{\pi}{2}, \frac{\pi}{2}\right]$. A uniform distribution of the rotations can be obtained with Euler angles, when a non-uniform

Figure 14. Illustration of 2D shape model building using (left) Procrustes analysis (PA) and (right) Continuous Procrustes analysis (CPA)

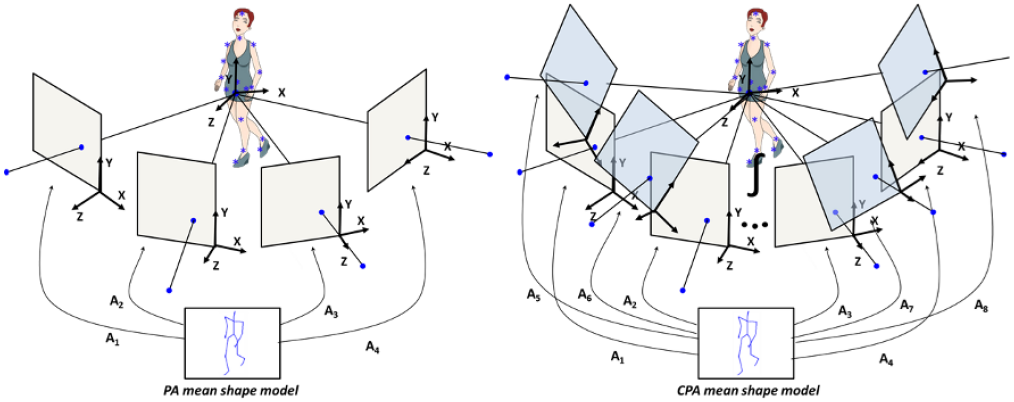

sampling of one of the three angles is used. However, angle and distribution depend on the Euler angles convention chosen, and there exist, at least, 24 conventions. In addition, despite of the uniform distribution, the gimbal lock problem persists while Euler angles are used.

Euler angles are also presented as an alternative to perform uniform rotations over continuous domains. Using the Haar measure into the integral definition the problem of discrete non-uniform distribution is avoided.

The use of quaternions can solve the previous problems while an appropriate parameterization is chosen. Presented results illustrate that Euler-to-quaternion conversion neither perform uniform distribution nor solves gimbal lock problem, despite of the use of quaternions. Axis-angle parameterization is also used to create unit quaternions, from uniformly distributed rotation axis and uniform rotation angle. However, this approach does not perform uniform rotations either.

Finally, it is checked that the method proposed in (Shoemake, 1992) results in uniform rotations. In this method, uniform unit quaternions are computed from three random variables. Therefore, this solution solves uniformity as well singularities.

FUTURE RESEARCH DIRECTIONS

2D shape models were introduced in the Chapter as state-of-the-art methods for object detection, image segmentation, and face tracking. The future research of non-biased 2D shape models is closely related with their possible applications in research fields such as improving Active Shape Models in the case of face detection.

Procrustes Analysis (PA) technique was also discussed. It is a state-of-the-art research area because of recent works about global optimization of PA. Hence, interesting research would be on the direction of global optimization of the, as well described, Continuous Procrustes Analysis (CPA). Other promising extensions of CPA would be a continuous formulation of PA using quaternions instead of Euler angles, and, independently of the parameterization of rotations, incorporating a subspace into the CPA formulation.

Finally, an additional research focus in the field of uniform sampling of SO(3) would be the uniform sampling of rotations in a limited part of the two-sphere using quaternions, since vectors rotated in the sphere are used to illustrate the orientations of a rotated object. The research on this subject would be useful to limit the rotations according to the problem at hands, avoiding memory resources and computational time.

CONCLUSION

The main goal of this chapter has been the study of the uniform sampling of rotations of 3D objects to be used on building unbiased 2D shape models. Along this work, standard non uniform rotations techniques over rotation group SO(3) were discussed, as well as uniform methods using both, Euler angles and quaternions, were presented. Moreover, the problem was addressed from discrete and continuous points of view. For the problem at hands, uniformity was checked trough the distribution of rotated couples of unit vectors into the unit 2-sphere S^2.

The concise review of the non-uniform sampling approaches discussed in this Chapter is that, on the one hand, Euler angles do not perform uniform rotations from a uniform sampling of the three angles and, in addition it is a parameterization that suffers singularities, i.e. the gimbal lock problem. On the other hand, these problems can be solved applying quaternions when correct parameterization is used; intuitive creation of unit quaternions as Euler angles conversion or angle-axis approach do not perform uniformly distributed rotations.

Three methodologies were presented to perform uniform rotations. The first solution to the problem was to use Euler angles. Uniformity is obtained for a certain distribution of one of the three angles, which depends on the convention that is being used; however, despite of uniform rotations, singularities are not solved with this method. The second approach consisted on using quaternions, following a methodology which generates uniform random unit quaternions from three random variables. In this case, uniform rotations are achieved, as well as problems related to singularities are solved. Finally, instead of general rotation methodologies, the third approach relied on the use of Continuous Procrustes Analysis (CPA), a particular method that builds unbiased 2D shape models from 3D objects. A continuous formulation of Euler angles was used in order to avoid non uniformity of rotations. This method does not solve problems related with Euler angles singularities. However, uniform rotations are performed and, in addition, CPA allows the possibility of limiting the rotations into a specific domain of the problem.

Each one of the three previous approaches performs uniform rotations. However, it is recommended to use each one of them according to the case to be applied. Uniform Euler angles are useful while intuitive rotations are needed, according to the axis of a basis. Otherwise, it is recommended to use other alternatives in order to avoid problems related with singularities and the rotation order, which varies depending on the convention of Euler angles. For the purpose of building unbiased 2D shape models from 3D objects, CPA presents similar performance that discrete Procrustes Analysis (PA), using a 2D dataset obtained by the use of uniform unit quaternions. The main differences are that CPA allows the use of limits over the sampling domain and unit quaternions solve not only uniform sampling, but also singularities.

ACKNOWLEDGMENT

This work is partly supported by the Spanish Ministry of Science and Innovation (projects TIN2011-28854-C03-01, TIN2009-14404-C02, CONSOLIDER INGENIO CSD 2007-00018) and the Comissionat per a Universitats i Recerca del Departament d'Innovació, Universitats i Empresa de la Generalitat de Catalunya.

REFERENCES

Baker, S., Matthews, I., & Schneider, J. (2004). Automatic construction of active appearance models as an image coding problem. *IEEE Transactions on Pattern Analysis and Machine Intelligence*, *26*(10), 1380–1384. doi:10.1109/TPAMI.2004.77

Bartoli, A., Pizarro, D., & Loog, M. (2010, August). *Stratified generalized procrustes analysis.* In British Machine and Vision Conference, Aberystwyth, UK.

Blanz, V., & Vetter, T. (1999, August). *A morphable model for the synthesis of 3D faces*. In International Conference and Exhibition on Computer Graphics and Interactive Techniques, Los Angeles, CA.

Cootes, T., Edwards, G., & Taylor, C. (2001). Active appearance models. *IEEE Transactions on Pattern Analysis and Machine Intelligence*, *23*(6), 681–685. doi:10.1109/34.927467

Cootes, T. F., & Taylor, C. J. (2001). *Statistical models of appearance for computer vision*. Retrieved from http://www.itu.dk/stud/projects_f2004/handtracking/referencer/Cootes%20den%20lange%20-%20app_model.pdf

De la Torre, F., & Nguyen, M. (2008, June). *Parameterized kernel principal component analysis: Theory and applications to supervised and unsupervised image alignment*. In IEEE Computer Vision and Pattern Recognition, Anchorage, AK.

Diaconis, P., & Shahshahani, M. (1987). The subgroup algorithm for generating uniform random variables. *Probability in the Engineering and Informational Sciences*, *1*(1), 15–32. doi:10.1017/S0269964800000255

Eggert, D., Lorusso, A., & Fisher, R. (1997). Estimating 3-D rigid body transformations: A comparison of four major algorithms. *Machine Vision and Applications*, *9*(5), 272–290. doi:10.1007/s001380050048

Gong, S., McKenna, S. J., & Psarrou, A. (Eds.). (2000). *Dynamic vision: From images to face recognition*. London, UK: Imperial College Press. doi:10.1142/p155

Goodall, C. (1991). Procrustes methods in the statistical analysis of shape. *Journal of the Royal Statistical Society. Series A, (Statistics in Society)*, *53*(2), 285–339.

Hamilton, W. R. S. (Ed.). (1853). *Lectures on quaternions*. Dublin, Ireland: Hodges and Smith.

Horn, B. K. P. (1987). Closed-form solution of absolute orientation using unit quaternions. *Journal of the Optical Society of America*, *4*(4), 629–642. doi:10.1364/JOSAA.4.000629

Igual, L., & De la Torre, F. (2010, June). *Continuous Procrustes analysis to learn 2D Shape models from 3D objects*. In Computer Vision and Pattern Recognition Workshops, San Francisco, CA.

Jones, M. J., & Poggio, T. (1989). Multidimensional morphable models. In *International Conference on Computer Vision*, Vol. 29, (pp. 683-688). Springer.

Kuffner, J. J. (2004). Effective sampling and distance metrics for 3D rigid body path planning. In *Proceedings of IEEE International Conference on Robotics and Automation, Vol. 4,* (pp. 3993-3998).

Kuipers, J. B. (Ed.). (1999). *Quaternions and rotation sequences: A primer with applications to orbits, aerospace and virtual reality*. Princeton, NJ: Princeton University Press.

Lerios, A. (1995). *Rotations and quaternions*. Technical Report. Retrieved from http://server2.phys.uniroma1.it/doc/giansanti/COMP_BIOPHYS_2008/LECTURES/LECT_2/Lerios1995.pdf

Mumford, D., & Shah, J. (1989). Optimal approximations by piecewise smooth functions and associated variational problems. *Communications on Pure and Applied Mathematics*, *42*(5), 577–685. doi:10.1002/cpa.3160420503

Naimark, M. A. (Ed.). (1964). *Linear representation of the Lorentz Group*. New York, NY: Macmillan.

Osher, S., & Paragios, N. (Eds.). (2003). *Geometric level set methods in imaging, vision, and graphics*. New York, NY: Springer.

Pizarro, D., & Bartoli, A. (2011). Global optimization for optimal generalized Procrustes analysis. In *IEEE Conference on Computer Vision and Pattern Recognition.* (pp. 2409-2415).

Shoemake, K. (1991). *Quaternions*. Tech Report. Retrieved from http://campar.in.tum.de/twiki/pub/Chair/DwarfTutorial/quatut.pdf

Shoemake, K. (1992). Uniform random rotations . In Kirk, D. (Ed.), *Graphics Gems III* (pp. 124–132). San Francisco, CA: Morgan Kaufmann.

Ullman, S., & Basri, R. (1991). Recognition by linear combinations of models. *IEEE Transactions on Pattern Analysis and Machine Intelligence*, *13*(10), 992–1006. doi:10.1109/34.99234

Yershova, A., Jain, S., LaValle, S. M., & Mitchell, J. C. (2010). Generating uniform incremental grids on SO (3) using the Hopf fibration. *The International Journal of Robotics Research*, *29*(7), 801–812. doi:10.1177/0278364909352700

ADDITIONAL READING

Arvo, J. (1992). Fast random rotation matrices . In Kirk, D. (Ed.), *Graphics Gems III* (pp. 117–120). San Francisco, CA: Morgan Kaufmann.

Dela Torre, F., & Black, M. J. (2003). Robust parameterized component analysis: Theory and applications to 2D facial appearance models. *Computer Vision and Image Understanding*, *91*(1), 53–71. doi:10.1016/S1077-3142(03)00076-6

Goodall, C. (1991). Procrustes methods in the statistical analysis of shape. *Journal of the Royal Statistical Society. Series A, (Statistics in Society)*, *53*(2), 285–339.

Górski, K. M., Hivon, E., Banday, A. J., Wandelt, B. D., Hansen, F. K., Reinecke, M., & Bartelmann, M. (2005). HEALPix: A framework for high-resolution discretization and fast analysis of data distributed on the sphere. *The Astrophysical Journal*, *622*, 759–771. doi:10.1086/427976

Hernández, A., Reyes, M., Escalera, S., & Radeva, P. (2010). *Spatio-temporal GrabCut human segmentation for face and pose recovery.* Computer Vision and Pattern Recognition, 2010, San Francisco, CA.

Kookinos, I., & Yuille, A. (2007, October) *Unsupervised learning of object deformation models*. In International Conference on Computer Vision, Rio de Janeiro, Brazil.

Miles, R. E. (1965). On random rotations in R^3. *Biometrika*, *52*(3-4), 636–639. doi:10.1093/biomet/52.3-4.636

Murnaghan, F. D. (1962). *The unitary and rotation groups. Lectures on applied mathematics*. Washington, DC: Spartan Books.

Pham, H. L., Perdereau, V., Adorno, B. V., & Fraisse, P. (2010). Position and orientation control of robot manipulators using dual quaternion feedback. In *Proceedings of IEEE/RSJ International Conference on Intelligent Robots and Systems* (pp. 658-663).

Ramamoorthy, S., Rajagopal, R., Ruan, Q., & Wenzel, L. (2006) Low-discrepancy curves and efficient coverage of space. In *Proceedings of Workshop on Algorithmic Foundations of Robotics* (pp. 203-218). Springer.

Rovira, J., Wonka, P., Castro, F., & Sbert, M. (2005). Point sampling with uniformly distributed lines. In *Proceedings of Point-Based Graphics: Eurographics/IEEE VGTC Symposium Proceedings* (pp. 109-118).

Sahu, S., Biswal, B. B., & Subudhi, B. (2008). A novel method for representing robot kinematics using quaternion theory. In *Proceedings of IEEE Sponsored Conference on Computational Intelligence, Control And Computer Vision In Robotics & Automation*.

Tomasi, C., & Kanade, T. (1992). Shape and motion from image streams under orthography: A factorization method. *International Journal of Computer Vision*, *9*(2), 137–154. doi:10.1007/BF00129684

KEY TERMS AND DEFINITIONS

Euler Angles: Representation of orientations in SO(3) through the composition of three rotations, each one around a single axis of a basis.

Landmark: Consistently labeled keypoint which represents an anatomical location of the model at hands.

Procrustes Analysis: Typical method to remove rigid transformations between shapes, composed by labeled landmarks, which minimizes the least-squared error between landmarks from training shapes.

Rigid Transformation: Transformation that preserves isometry, i.e. distances between every pair of points are preserved. Typical rigid transformations are rotation, translation, and isomorphic scaling.

Shape: Finite set of landmarks whose geometrical information remains unchanged when the shape suffers rigid transformations.

Statistical Shape Models: Models which are able to modify their shape according to the different transformations present in a training set.

Unit Quaternion: Point in the unit 3-sphere $S^3 \in \mathbb{R}^4$, which represents a rotation in SO(3).